

## On the glass temperature under extreme pressures

A. Drozd-Rzoska, S. J. Rzoska, and M. Paluch

*Institute of Physics, Silesian University, ul. Uniwersytecka 4, 40-007 Katowice, Poland*

A. R. Imre

*KFKI Atomic Energy Research Institute, H-1525 Budapest, POB 49, Hungary*

C. M. Roland

*Chemistry Division, Naval Research Laboratory, Code 6120, Washington DC 20375-5342*

(Received 21 November 2006; accepted 8 March 2007; published online 25 April 2007)

The application of a modified Simon-Glatzel-type relation [Z. Anorg. Allg. Chem. **178**, 309 (1929)] for the pressure evolution of the glass temperature is presented, namely,  $T_g(P) = T_g^0 [1 + \Delta P / (\pi + P_g^0)]^{1/b} \exp[-(\Delta P/c)]$ , where  $(T_g^0, P_g^0)$  are the reference temperature and pressure,  $\Delta P = P - P_g^0$ ,  $-\pi$  is the negative pressure asymptote,  $b$  is the power exponent, and  $c$  is the damping pressure coefficient. The discussion is based on the experimental  $T_g(P)$  data for magmatic silicate melt albite, polymeric liquid crystal P8, and glycerol. The latter data are taken from Cook *et al.* [J. Chem. Phys. **100**, 5178 (1994)] and from the authors' dielectric relaxation time ( $\tau(P)$ ) measurements, which employs the novel pressure counterpart of the Vogel-Fulcher-Tammann equation:  $\tau(P) = \tau_0^P \exp[D_P \Delta P / (P_0 - P)]$ , where  $\Delta P = P - P_{SL}$  ( $P_{SL}$  is the stability limit hidden under negative pressure),  $P_0$  is the estimation of the ideal glass pressure, and  $D_P$  is the isothermal fragility strength coefficient. Results obtained suggest the hypothetical maximum of the  $T_g(P)$  curve, which can be estimated due to the application of the supporting derivative-based analysis. A hypothetical common description of glass formers characterized by  $dT_g/dP > 0$  and  $dT_g/dP < 0$  coefficients is suggested. Finally, the hypothetical link between molecular and colloidal glass formers is recalled. © 2007 American Institute of Physics. [DOI: [10.1063/1.2721044](https://doi.org/10.1063/1.2721044)]

### I. INTRODUCTION

Over the last decade the application of hydrostatic pressure has become a prominent strategy for resolving the glass transition puzzle.<sup>1-4</sup> The advantage of pressure is due to the fact that temperature effects are coupled both to the activation energy and density changes, whereas pressure solely affects density.<sup>2,3</sup> Consequently, experimental studies involving both pressure ( $P$ ) and temperature ( $T$ ) can constitute a fundamental reference for theoretical models.<sup>1-4</sup> Unfortunately, pressure studies of the glass transition employing state-of-the-art modern techniques are still limited.<sup>2-14</sup> A fundamental requisite step in the interpretation of such data is a simple and reliable parametrization of the pressure evolution of the glass temperature  $T_g(P)$ . It is also worth recalling that the  $dT_g/dP$  coefficient is included into the Ehrenfest equations<sup>15</sup> or the Prigogone-Dufay ratio.<sup>15,16</sup> Hence, the  $T_g(P)$  behavior has an important influence on properties under atmospheric pressure. Regarding applications, noteworthy is the pressure induced amorphization phenomenon<sup>17-20</sup> or the significance of a simple  $T_g(P)$  parametrization for deep Earth, volcanology, and planetary sciences.<sup>21,22</sup>

The overwhelming majority of experimental data indicate the increase of  $T_g$  on compressing, coupled with decreasing value of the  $dT_g(P)/dP$  coefficient.<sup>2-14</sup> Notwithstanding, until recently, the  $T_g(P)$  data have been portrayed mainly by a second order polynomial,<sup>2,3,6,9,11</sup>

$$T_g(P) = T_g^0 + AP + BP^2, \quad (1)$$

where  $A > 0$  and  $B < 0$  are fitted parameters.

Only in 1998 Andersson and Andersson<sup>10</sup> postulated another relation, which has gained a great popularity in the following years,<sup>2,3,6,7,11-14</sup>

$$T_g(P) = T_g^0 \left( 1 + \frac{P}{\Pi} \right)^{1/b}, \quad (2)$$

where  $T_g^0(P)$  is the reference temperature, usually taken as the glass temperature for the ambient pressure, and  $\Pi$  and  $b$  are adjustable parameters.

However, the theoretical analysis by DiMarzio *et al.*,<sup>23</sup> Bantzelius *et al.*,<sup>24</sup> and Skorudonov and Godovskii<sup>25</sup> suggested that on compressing the permanent decrease of  $dT_g/dP > 0$  is followed by the appearance of a high temperature asymptote, i.e., approaching the condition  $dT_g/dP \rightarrow 0$  for high enough pressures. Additionally, Donth<sup>1</sup> suggested that a high temperature asymptote ( $\theta$ ) along with a negative pressure asymptote ( $-\pi$ ) should be expected for  $T_g(P)$  parametrization. Subsequently, based on the Williams-Landolt-Ferry equation for changes of viscoelastic properties on approaching the glass transition, the following relation was derived:<sup>1,26,27</sup>

$$T_g(P) = \frac{C}{P - \pi} + \theta. \quad (3)$$

Unfortunately, its application is limited to few polymeric glass formers.<sup>26,27</sup> In the opinion of the authors this can be linked to the fact that fitting values of  $C$ ,  $\pi$ , and  $\theta$  parameters are ambiguous due to the usually weakly nonlinear  $T_g(P)$

experimental dependences. Unfortunately, neither Eq. (1) nor Eq. (2) can yield the mentioned asymptotic behavior. Recently, it was noted that Eq. (2), in fact, parallels the Simon-Glatzel (SG) relation<sup>28</sup> well established for decades for describing the evolution of the melting temperature  $T_m(P)$ .<sup>29-34</sup> Recently, a modified SG-type (mSG) equation for the pressure evolution of the glass transition was proposed, namely,<sup>9</sup>

$$T_g(P) = F(P)D(P) = T_g^0 \left(1 + \frac{\Delta P}{\Pi}\right)^{1/b} \exp\left(-\frac{\Delta P}{c}\right), \quad (4)$$

where  $\Delta P = P - P_g^0$ , values of  $T_g^0$  and  $P_g^0$  are the correlated reference pressure and temperature,  $c$  is the damping coefficient,  $F(P)$  denotes the rising term related to the SG-type equation, and  $D(P)$  is the damping term.

Equation (4) can yield the negative pressure asymptote ( $-\pi$ ) for  $T_g^0 \rightarrow 0$  as well as the high temperature asymptote ( $\theta$ ) for the proper selection of the damping coefficient. However, when discussing the general pattern for  $T_g(P)$  evolution, two important facts should be pointed out. Firstly, there is no clear experimental evidence for the temperature  $\theta$  asymptote, to the best of the authors' knowledge. Secondly, for a few atypical glass formers such as ionic liquids,<sup>35</sup> magnetic silicate melts,<sup>36</sup> or paraelectric crystals,<sup>37,38</sup> the opposite behavior, i.e.,  $dT_g/dP < 0$ , were reported, which contradicts the appearance of the  $\theta$  asymptote, in the opinion of the authors. Consequently, the following questions arise: (i) Is a general pattern of  $T_g(P)$  evolution, valid for glass formers characterized both by  $dT_g(P)/dP > 0$  and  $dT_g(P)/dP < 0$ , possible? (ii) Why are glass formers characterized by  $dT_g(P)/dP < 0$  so rare?

This paper focuses on preliminary answers to these questions. The discussion presents a novel, derivative-based method for predicting  $T_g(P)$  evolution based on Eq. (4). The analysis is focused on glycerol, for which the most extensive set of  $T_g(P)$  data seems to exist.<sup>39-42</sup> Subsequently, the  $T_g(P)$  behavior in P8 polymeric liquid crystal,<sup>11</sup> where  $dT_g(P)/dP \rightarrow 0$  for  $P \rightarrow 0.5G$  Pa, and in the magmatic silicate melt albite,<sup>36</sup> where  $dT_g(P)/dP < 0$ , is discussed. Available experimental  $T_g(P)$  data for glycerol were supplemented based on a dielectric relaxation time analysis. The latter used the novel pressure counterpart of the Vogel-Fulcher-Tammann (VFT) equation, enabling an insight into the negative pressure domain.

## II. ESTIMATION OF THE GLASS TEMPERATURE

There is a set of thermodynamic and dynamic experimental techniques which can be used for determining the glass temperature under atmospheric pressure.<sup>1</sup> However, experimental implementations of these experimental methods for pressurized glass formers are strongly limited. In practice, they are focused on the evolution of dynamic properties, such as viscosity ( $\eta$ ) or dielectric relaxation time ( $\tau$ ), based on empirical conditions  $\eta(T_g, P_g) = 10^{13}P$  or  $\tau(T_g, P_g) = 100$  s.<sup>1-14</sup> Most often, values of  $(T_g, P_g)$  are taken from the extrapolation via the VFT dependence, namely,<sup>1-14</sup>

$$\tau(T) = \tau_0 \exp\left(\frac{D_T T_0}{T - T_0}\right), \quad P = \text{const}, \quad (5)$$

where  $D_T$  is the fragility strength coefficient and  $T_0$  is the estimation of the ideal glass temperature. The prefactor  $\tau_0$ , usually of the order of  $10^{14 \pm 2}$  s, reflects the relaxation time near the high temperature stability limit for the given material.

However, in the practice of pressure studies the isothermal pressure evolution of dynamic properties is most often tested.<sup>2-14</sup> Since such investigations are usually limited to the moderate pressure domain, the question of a simple and reliable extrapolation beyond the experimentally available pressures appears. In the last decade, most often, the pressure counterpart of Eq. (5),<sup>5</sup> called the PVFT relation, was used,<sup>2-14</sup>

$$\tau(P) = \tau_0^P \exp\left(\frac{D_P P}{P_0 - P}\right), \quad T = \text{const}, \quad (6)$$

where  $D_P$  is the isothermal fragility coefficient and  $P_0$  is the estimation of the ideal glass pressure.

It was shown before<sup>8</sup> that obtaining the ultimate set of parameters in Eqs. (5) and (6) can be supported by the derivative-based analysis. Namely, for the VFT [Eq. (5)]<sup>8</sup>

$$\left[\frac{d \ln \tau}{d(1/T)}\right]^{-1/2} = (H'_a)^{-1/2} = [(D_T T_0)^{-1/2}] - \frac{[T_0(D_T T_0)^{-1/2}]}{T} = A - \frac{B}{T}, \quad (7)$$

where  $H'_a$  is the measure of the apparent activation enthalpy.

Hence, the plot  $(H'_a)^{-1/2}$  yields a linear dependence from which values of  $D_T = 1/AB$  and  $T_0 = B/A$  can be obtained. For Eq. (6) a similar derivative analysis yields<sup>8</sup>

$$\left[\frac{d \ln \tau}{dP}\right] = [V'_a]^{-1/2} = (D_P P_0)^{-1/2} P_0 - (D_P P_0)^{-1/2} P = A - BP, \quad (8)$$

where  $V'_a$  is the measure of the apparent activation volume.

In this case the linear regression also yields values of basic parameters, namely,  $P_0 = A/B$  and  $D_P = 1/AB$ . Noteworthy is the significant difference between Eqs. (6) and (5). For the VFT [Eq. (5)] the prefactor  $\tau_0$  is related to the high temperature behavior, which terminates at the liquid-vapor stability limit. For the PVFT [Eq. (6)] the prefactor  $\tau_0^P$  is linked to the relaxation time under atmospheric pressure for the given temperature. Hence, it can take an arbitrary value ranging from seconds to picoseconds.<sup>2-14</sup> In the opinion of the authors, one should expect a similar physical meaning of prefactors in the VFT equation and of its pressure counterpart. To resolve this puzzle, the following dependence may be proposed:

$$\tau(P) = \tau_0^P \exp\left[\frac{D_P \Delta P}{P_0 - P}\right] = \tau_0^P \exp\left[\frac{D_P P - D_P P_{SL}}{P_0 - P}\right], \quad (9)$$

where  $\Delta P = P - P_{SL}$  and  $P_{SL}$  is a liquid-vapor (LV) stability limit.

Then, the linearized, derivative-based transformation of data yields

$$\left[ \frac{d \ln \tau}{dP} \right] = [V'_a]^{-1/2} = [D_P(P_0 - P_{SL})]^{-1/2} P_0$$

$$-[D_P(P_0 - P_{SL})]^{-1/2} P = A + BP. \quad (10)$$

In this case  $A/B = P_0$ ,  $1/AB = D_P P_0 / (P_0 - P_{SL})$ , and  $P_{SL} < 0$ . Hence, fits using the former PVFT [Eq. (6)] and the present PVFT [Eq. (9)] are linked to the same value of  $P_0$  but to different values of the fragility strength coefficients, namely,  $D_P^{\text{new}}/D_P^{\text{old}} = (P_0 - P_S)/P_0$ . For Eq. (9) the prefactor  $\tau_0^P$  reflects the relaxation time at  $P = P_{SL}$ , i.e., at the LV stability limit. The existence of the LV stability limit within the negative pressure domain is well documented for a variety of liquids.<sup>43</sup> Unfortunately, studies of glass forming systems within the negative pressure domain are still at the very beginning despite the strongly suggested significance of such results for vitrifying systems.<sup>1,43-48</sup>

In the opinion of the authors, Eq. (9) may be considered as a possible tool for estimating the location of the LV stability limit loci from experimental data within the experimentally available positive pressure domain. When approaching the glass transition either by pressure or by temperature paths, two dynamical domains appears.<sup>2,3,8,11-14</sup>

The crossover occurs at the so-called “magic,” universal time scale located near  $\tau(T_B, P_B) = 10^{-7 \pm 1}$  s.<sup>49</sup> They are related to the different set of parameters in the VFT or PVFT equations.<sup>8</sup> For the estimation of the real glass temperature for the given glass former, only the data located within the low temperature ( $T < T_B$ ) or high pressure ( $P > P_B$ ) dynamical domain should be taken into account.<sup>8</sup> In practice, only these dynamical domains are available for broadband dielectric spectroscopy (BDS), which was used for estimating additional  $T_g(P)$  data for glycerol. This is associated with the fact that the high pressure implementation of BDS is restricted to frequencies  $f < 10$  MHz.<sup>2-14</sup>

Figure 1 shows the pressure evolution of the primary relaxation time in glycerol for a selected isotherm. BDS measurements were carried out on a Novocontrol BDS 40 spectrometer, using the pressure setup described elsewhere.<sup>3,8</sup> The relaxation time was determined from peak frequencies ( $f_p$ ) of loss curves via relation  $\tau = 1/2\pi f_p$ .<sup>1-3</sup> The inset shows the results of the derivative-based transformation [see Eqs. (8) and (10)] of the experimental data. The results were subsequently used as input parameters to PVFT [Eqs. (6) and (9)]. The solid curve in Fig. 1 is linked to the resulting parametrization by Eq. (6) and the dashed curve is related to Eq. (9). Both PVFT relations yield the same values of the “ideal glass pressure estimate”  $P_0$  and the glass pressure  $P_g$  for the given temperature. However, the novel PVFT [Eq. (9)] can be extended into the negative pressure domain down to  $P_{SL} \approx -0.38$  GPa. It is noteworthy that for this pressure the relaxation time  $\tau = \tau_0^P$  is close to the mentioned magic time scale. Also, we should mention here that, for example, for water, the deepest value for the thermodynamic liquid-vapor stability limit (predicted by different models) is

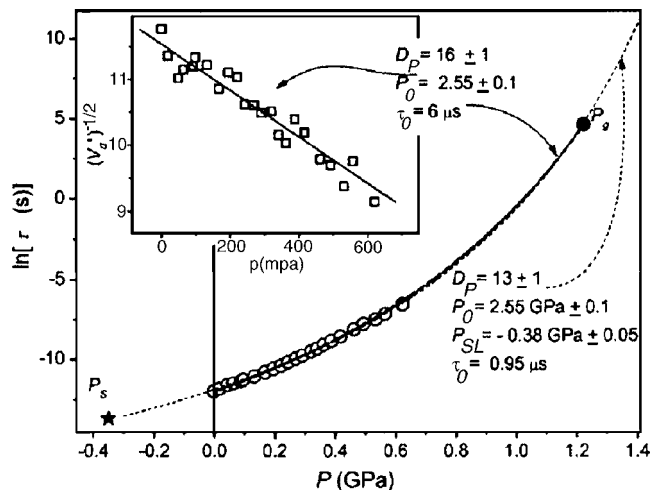


FIG. 1. The evolution of dielectric relaxation time in pressurized glycerol for  $T=244$  K isotherm. The solid curve is for the “old” PVFT [Eq. (6)] and the dashed curve is for the “novel” PVFT [Eq. (9)]. The solid circle indicates the extrapolated glass transition point from the condition  $\tau(T_g, P_g) = 100$  s. The star points out the extrapolated negative pressure stability boundary. The fits via the pressure counterpart of the VFT dependence [Eqs. (6) and (9)] were supported by parameters from the derivative-based analysis shown in the inset [Eqs. (8) and (10)].

located between  $-0.2$  and  $-0.4$  GPa,<sup>43</sup> suggesting that the value obtained here might be in a good order of magnitude and not unrealistically high or low.

### III. THE PRESSURE EVOLUTION OF THE GLASS TEMPERATURE

Glycerol can be considered as one of the most classical low molecular glass forming liquids, for which probably the most extensive set of  $T_g(P)$  data is available.<sup>1</sup> In 1972 Johari and Whalley<sup>39</sup> reported the increase of  $T_g$  and the gradual decrease of  $dT_g(P)/dP$  when pressuring up to  $P=5.3$  GPa. In 1994 Cook *et al.*<sup>40</sup> reported superior  $T_g(P)$  data up to  $P = 12$  GPa, which was obtained using viscosity measurements. These results are in fair agreement with the ones reported by Schulte and Oliver III,<sup>41</sup> who concluded that “a continuous decrease in  $T_g(P)/dP$  is observed up to about 3.5 GPa above which a nearly constant value of 18.2 K/GPa is observed” based on BDS measurements. The same technique was used by Reiser *et al.*<sup>42</sup> in measurements up to 700 MPa. They also reported the gradual decreases of  $T_g(P)$  with pressuring and suggested another, presumably linear, pressure dependence above 1 GPa.

In the discussion of the  $T_g(P)$  behavior in glycerol presented below, we used data from Cook *et al.*,<sup>40</sup> supplemented by data of Reiser *et al.*<sup>42</sup> for  $P < 0.5$  GPa, and several points obtained from the authors’  $\tau(T, P)$  measurements, via the  $\tau(T_g, P_g) = 100$  s condition. For portraying  $T_g(P)$  evolution, shown in Fig. 2, the modified SG-type equation [Eq. (4)] was applied. It can be easily shown that for the negligible damping term, i.e.,  $c^{-1} = 0$ , Eq. (4) is linked to the linear pressure dependence for the derivative-based transformation of data, namely,  $[d(\ln T_g)/dP]^{-1} = A + BP$ .<sup>9</sup> The subsequent linear regression of data can give the power exponent  $b=B$  and the negative pressure asymptote for  $T_g^0 \rightarrow 0$ , namely,  $\pi = A/B$ . The latter can be associated with the “disposable pressure”

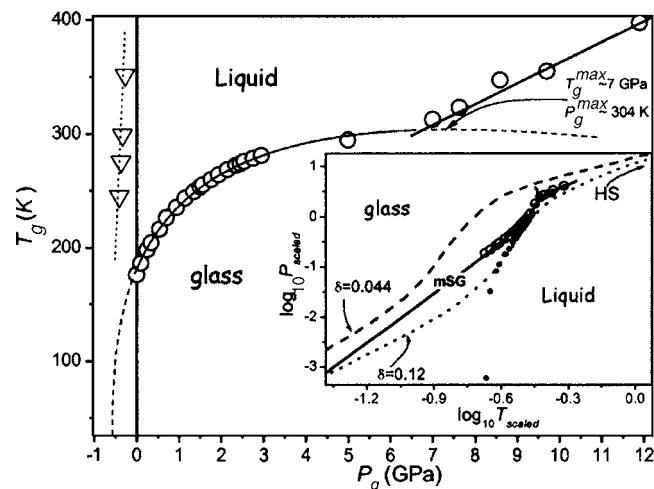


FIG. 2. The pressure evolution of the glass temperature in glycerol. Experimental data (open circles) have been taken from Cook *et al.* (Ref. 40) and from the authors' measurements. The solid curve shows the parametrization of experimental data via Eq. (4), with parameters determined in the derivative-based transformation of experimental data given in Fig. 3. The solid straight line portraying data at extreme pressure can be described by the linear dependence with  $dT_g/dP \approx 18.2$  K/GPa (Ref. 41). The extrapolations beyond the experimental domain are shown by the dashed curve and the dashed line. The dotted line in the negative pressure domain shows the estimated loci of the hypothetical stability limit. The inset recalls the square-well (SW) model and the MCT based analysis of the glass transition evolutions. Data presented here in SW model units, namely, for glycerol:  $P_{\text{scaled}} = P_g/3.09$  GPa and  $T_{\text{scaled}} = P_g/826$  K (Ref. 63). The dashed and the dotted curve, linked to the attraction parameter given in the inset, and the solid circles associated with  $P_g(T_g)$  for glycerol parallel results given in Fig. 1 in Ref. 63. The open circles are also for glycerol, but assuming the negative pressure asymptote as the reference. The solid curve and the solid line reflect the parametrization of  $T_g$  vs  $P_g$  discussed in the main part of Fig. 2.

coefficient by  $\Pi = \pi + P_g^0$ . If the damping term cannot be neglected in Eq. (4), one may expect that for the optimal selection of the damping coefficient  $c$

$$\left[ \frac{d \ln T_g}{dP} + c^{-1} \right]^{-1} = A + BP. \quad (11)$$

The plot of  $T_g(P)$  transformed in this way should follow a linear pressure dependence yielding  $\pi = A/B$ ,  $b = B$ , and  $c$  parameters. It is noteworthy that parameters in the basic Simon-Glatzel-type equation applied for melting curves<sup>28</sup> as well the Andersson and Andersson equation<sup>10</sup> were always considered as empirical, pressure dependent disposable coefficients.<sup>2-14,28-34</sup> The above discussion points out that in any Simon-Glatzel-based equation the optimal set of pressure invariant coefficients can be determined.

Figure 3 shows results of the derivative-based analysis of the  $T_g(P)$  data for glycerol. The  $b$ ,  $\pi$ , and  $c$  parameters obtained in this way were next substituted into Eq. (4), yielding the solid curve portraying  $T_g(P)$  in Fig. 2. The derivative-based analysis via Eq. (11) indicates the domain of validity of the modified SG relation prior to the final parametrization. For glycerol it obeys  $P < 5$  GPa. However, the same set of  $b$ ,  $\pi$ , and  $c$  parameters may be estimated even basing on a smaller pressure domain because they are pressure invariant. Figure 2 shows that Eq. (4) with the above set of parameters yield a fairly well description of experimental data up to  $P \approx 6.5$  GPa. The resulting parametrization shows

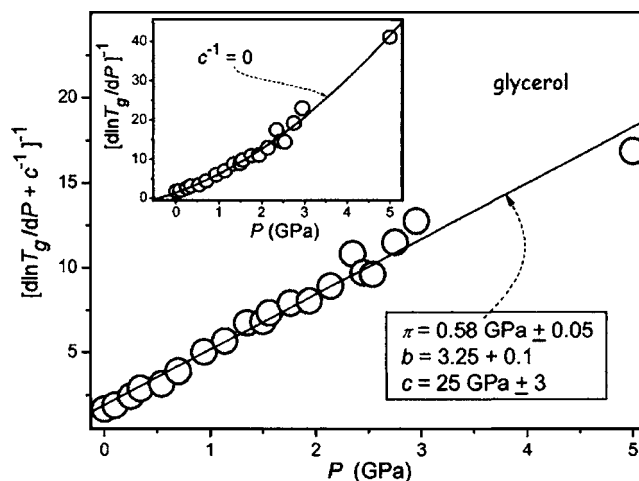


FIG. 3. The derivative-based transformation of the  $T_g(P)$  data using Eq. (11) yielding parameters for the extended SG-based relation in glycerol from the linear regression analysis. They have been applied for portraying  $T_g(P)$  data in Fig. 1. The inset shows the behavior of transformed data without the damping term.

the gradual decrease of the  $dT_g(P)/dP$  coefficient from approximately 88.6 K/GPa at  $P=0.1$  MPa to approximately 2 K/MPa for  $P \rightarrow 6.5$  GPa. For  $P > 6.5$  GPa the discussed behavior can be portrayed by  $T_g(P) \propto P^x$ . The direct analysis in the main plot suggests the linear behavior ( $x=1$ ), but the log-log plot in the inset may suggest that  $0.3 < x \leq 1$ . The solid straight line for very high pressures in Fig. 2 represents the linear behavior described by  $dT_g(P)/dP = 18.2$  K/GPa, suggested by Schulte and Oliver III<sup>41</sup> for  $P > 3.5$  GPa. It is visible that such dependence fairly follows the  $T_g(P)$  data, but for  $P > 6.5$  GPa. The dotted line shows the estimated location of the stability limit hidden in the negative pressure domain, obtained due to the novel PVFT [Eq. (9)]. The parametrization via the mSG [Eq. (4)] estimates the negative pressure asymptote at  $-\pi \approx 0.55$  GPa and indicates the hypothetical maximum of the  $T_g(P)$  curve, i.e., the crossover between  $dT_g(P)/dP > 0$  to  $dT_g(P)/dP < 0$  domains at  $P_{\text{max}}(T_{\text{max}} \approx 304 \text{ K}) \approx 7$  GPa. This maximum is located in the experimentally nonavailable pressure domain since for  $P_g > 6.5$  GPa the mentioned (almost) linear increase of  $T_g$  on compressing occurs.

Figure 4 presents the glass temperature behavior for the hairy rod macromolecule poly(*p*-phenylene) with sulfonate ester and dodecyl side chain (P8),<sup>11</sup> a material for which a rough analysis of the  $T_g(P)$  data suggested  $dT_g(P)/dP \rightarrow 0$  on compressing. P8 is a polymeric liquid crystal (LC), which vitrifies in the LC mesophase, well below the clearing temperature.<sup>11</sup> The inset presents results of our analysis which yields the negative pressure asymptote  $-\pi \approx -0.25$  GPa and exponent  $b \approx 2.4$ . Using these parameters, the experimental data can be very well described, as seen in the main part of Fig. 4. Noteworthy is the appearance of a hypothetical maximum already at  $P_{\text{max}}(T_{\text{max}} = 438 \text{ K}) \approx 0.6$  GPa.

Experimental  $T_g(P)$  data for materials characterized by  $dT_g(P)/dP < 0$  are extremely rare. Figure 5 shows such results for a magmatic silicate melt albite.<sup>36</sup> Although in this case the derivative-based analysis is not possible because of

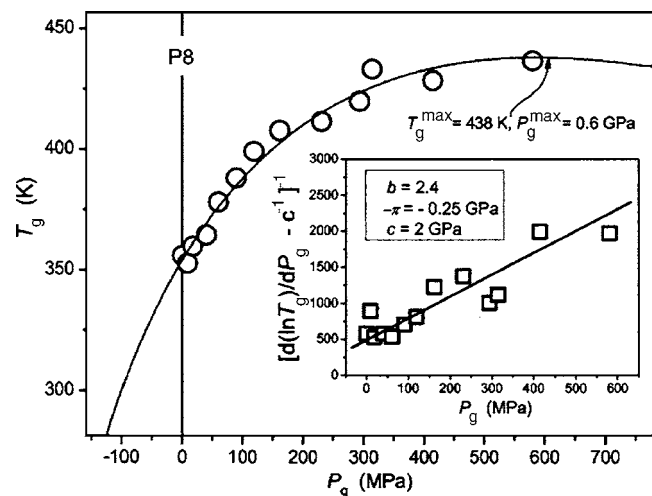


FIG. 4. The parametrization of the pressure dependence of the glass temperature in liquid crystalline polymer P8.  $T_g(P)$  data are taken from Gitsas *et al.* (Ref. 11). The inset shows results of the derivative-based transformation for the optimal value of the damping coefficient via Eq. (11). The solid curve in the main plot represents Eq. (4) with fitting parameters given in the inset.

the limited number of  $T_g(P)$  points, direct fitting via Eq. (4) revealed the existence of the negative pressure asymptote and a maximum in  $T_g(P)$ , hidden below  $P=0$ . This suggests that by the isotropic stretching albite can be converted into a “normal” glass forming liquid characterized by  $dT_g/dP > 0$ , although we should mention that the expected  $-2.1$  GPa value is much deeper than the deepest experimentally accessible values for various liquids,<sup>43</sup> but still smaller than the expected stability limit for similar glass forming materials.<sup>18,50</sup>

#### IV. CONCLUSIONS

First, we would like to recall the novel pressure counterpart of the VFT equation which, supported by the derivative-based transformation, can be used not for estimating coordinates of the vitrification point, the ideal glass VFT point, and the speculative estimation of the stability limit hidden in the

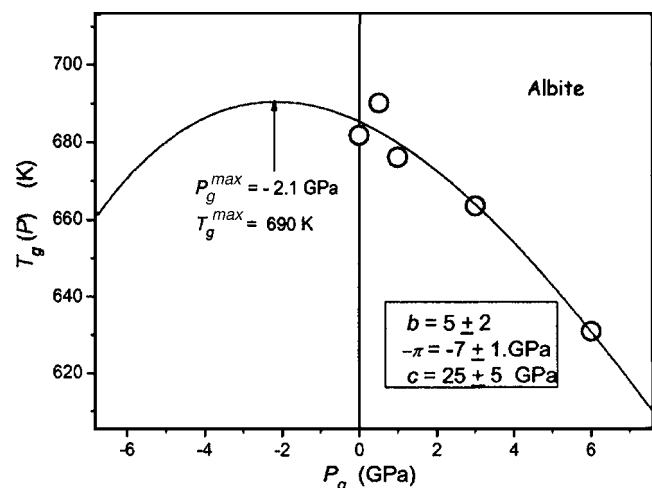


FIG. 5. The pressure evolution of the glass temperature in albite (Ref. 32). The solid curve is the fit of Eq. (4). Note that the hypothetical maximum of  $T_g(P)$  is hidden in the negative pressure domain.

negative pressure domain. To the best of the authors’ knowledge there are no practical proposals for extending the evolution of dynamic properties into the challenging domain so far.<sup>51</sup> Subsequently, a mSG-type relation [Eq. (4)] was introduced for portraying the pressure evolution of glass temperature in selected glass formers. The application of the additional derivative-based analysis [Eq. (11)] made it possible to obtain an optimal set of relevant parameters. The applied procedure yielded a negative pressure asymptote and pointed out a hypothetical maximum of  $T_g(P)$ . The latter can be hidden due to the appearance of yet another pressure dependence of  $T_g(P)$  at high enough pressures (glycerol) or due to its location in the negative pressure domain (albite). The presented analysis may suggest a common description of materials characterized by  $dT_g(P)/dP > 0$  and  $dT_g(P)/dP < 0$  under atmospheric pressure, which have not been pointed out so far, to the best of the authors’ knowledge.

However, it can be suspected that the maximum of  $T_g(P)$  appears just at the end of the data range. For example, one could assume that the mSG relation simply breaks down at extreme pressures, without assigning a special meaning to this point. However, the following arguments may support the hypothetical  $T_g(P)$  maximum in some glass formers: (i) There is a clear experimental evidence for the maximum for melting curves  $T_m(P)$ . (ii) The glass temperature and the melting temperature are correlated; namely,  $T_g/T_m \geq 2/3$  under atmospheric pressure for “good” glass formers is expected. This may suggest a similar pressure evolution of  $T_g(P)$  and  $T_m(P)$ . (iii) Equation (4) is governed by pressure invariant coefficients  $c$ ,  $b$ , and  $\pi$  ( $\Pi = \pi + P_g^0$ ), which supports the validity of extrapolation beyond the experimentally available domain of pressures. (iv) The latter issue supports results of melting curves, which includes materials showing the crossover from  $dT_m(P)/dP > 0$  to  $dT_m(P)/dP < 0$ .<sup>31</sup> This phenomenon was first noted in rubidium,<sup>52</sup> cesium,<sup>53</sup> and, next, in few other materials,<sup>36,54</sup> including polymeric ones.<sup>55</sup> (iv) The evidence of the  $T_g(P)$  experimental data available so far is still very limited, regarding the number of materials and the range of pressures.<sup>56</sup>

The possible appearance of the maximum for  $T_g(P)$  may suggest that on compressing for some glass formers the sequence: *supercooled liquid* [ $dT_g(P)/dP > 0$ ]—*glass*—*reentrant supercooled liquid* [ $dT_g(P)/dP < 0$ ] may occur. This means that materials characterized by  $dT_g/dP < 0$ , for instance, albite in Fig. 5, can already be in the *reentrant liquid state* under atmospheric pressure. However, this  $T_g(P)$  evolution is restricted by the stability limit in the negative pressure domain and by yet another pressure  $T_g(P)$  dependence appearing at extreme pressures.

In fact, the liquid—glass—reentrant liquid sequence has already been noted in colloidal suspensions with polymer-mediated interaction<sup>57</sup> and in micelle-polymer mixtures,<sup>58</sup> although only as a function of temperature or concentration. A theoretical basis for this phenomenon was proposed by Sciortino.<sup>59</sup> According to his model, during the cooling of normal glass formers, particles become progressively more hindered due to the presence of neighbors and finally become “caged” in the solid amorphous state. In this glassy state, particles can only rattle within their cages. However, in the

presence of a dominated attractive interaction, particles can adhere to one another, shrinking the cage size and simultaneously yielding a more inhomogeneous distribution of an empty space. These empty regions can form channels through which particles can diffuse, whereby the glass melts on further cooling, yielding a reentrant colloidal liquid. The eventual transformation to the subsequent, so-called attractive glass may next appear.<sup>58,59</sup>

One may speculate that the pressurization can partially substitute the attractive interaction, also leading to the reentrant liquidization. Unfortunately, there is no pressure studies on a colloid-polymer (CP) mixture so far related to this phenomenon. However, when changing the concentration of the solvent, one can control the effective temperature and the density of the colloid which can be interpreted as a study under varying temperature and pressure. Nevertheless, a question arises whether the link between CP mixtures and molecular glasses exists.<sup>1,60–62</sup> Fortunately, Voigtmann and Poon<sup>63</sup> recently published probably the first ever paper clearly related to this issue, moreover focusing on the pressure evolution of the glass temperature. It is based on the analysis via the square-well (SW) model and the mode-coupling theory (MCT) which, despite its relative simplicity, are known to portray reasonably the glassy dynamics of CP mixtures.<sup>1,62,63</sup> The inset in Fig. 2 partially recalls key results from Ref. 63: (a) The dotted and the dashed curves are the MCT predictions for the SW vitrifying system with the given attraction range parameter  $\delta$ , i.e.,  $U(r) = -U_0$  for  $d < r < d(1 + \delta)$ ,  $U(r) = \infty$  for  $d < r$ , and  $U(r) = 0$  elsewhere;  $r$  is the hard core radius and  $d$  is for the distance. (b) For the SW model an equation of state was built. This made it possible to scale experimental data for the CP mixture from the available density-concentration plane<sup>57</sup> into the  $P$ - $T$  plane. The  $P_g(T)$  data scaled in this way fairly well coincide with the dashed curve for  $\delta = 0.044$ , from  $P_{\text{scaled}} \approx 0.04$  to  $P_{\text{scaled}} \approx 1$ .<sup>63</sup> (c) At the same plot in Ref. 63 the  $T_g(P)$  experimental data scaled to the SW model units for few molecular liquids, including glycerol, were placed. In Ref. 63 all these data were grouped at the model curve for  $\delta = 0.12$  near  $T_{\text{scaled}} \approx 0.3$ , with a “generic drop” for  $T_{\text{scaled}}$  approaching 0.2. In the inset in Fig. 2 this unique behavior is shown for the glycerol data from the main plot by solid circles.

Subsequently, three domains for pressurized glass formers were pointed out in Ref. 63: “(A)  $P_{\text{scaled}} \geq 1$  where the glass-transition temperature is linear in  $T$ , i.e., it follows hard-sphere isochore, (B)  $0.1 \leq P_{\text{scaled}} \leq 1$  where  $P_g(\log T)$  exhibits an almost vertical steep increase with  $\log T$ . One can call this a ‘temperature driven’ section..., (C) reflecting a dilute system of sticky hard spheres.”

The comparison of theoretical, transformed colloidal and molecular glasses leads to the conclusion that regime (C) is never entered for molecular liquids.<sup>63</sup> To understand the mentioned generic drop of the glass transition line for molecular liquids, a need for the novel theory was postulated in Ref. 63.

In our opinion the mention of generic drop is the parasitic artifact associated with the definition of pressure starting from  $P = 0$  and the applied log-log scale. For liquids passing  $P = 0$  do not introduce any singularity.<sup>43</sup> The existing

preliminary experimental evidence clearly shows that  $T_g(P)$  can be smoothly extended into the negative pressure domain.<sup>44,45</sup> In the inset in Fig. 2 the same, SW model scaled, data for glycerol are shown, but taking the negative pressure asymptote  $P = -\pi$  and the mSG relation (4) as the reference. This is shown by open circles. Solid lines are for Eq. (4) ( $P_g < 6.5$  GPa) and for additional pressure dependence at  $P_g > 6.5$  GPa. No universal generic drop for molecular glass formers near  $P = 0$  appears. The behavior of the CP mixture and glycerol are now more than what is suggested in Ref. 63. For glycerol, and one may assume that for other molecular glass former, the glass transition dependence can be extended into the “dilute” domain (C). One may expect that this will be limited by the intersection with the stability limit (spinodal) line which may be expected near  $P_{\text{scaled}} \approx 0.02$ . The corrected experimental scaled data for glycerol are located between theoretical model curves calculated for  $\delta = 0.04$  and  $\delta = 0.12$ . In the inset in Fig. 2 the extension of the mSG based curve above the hypothetical maximum is also shown. Although in Ref. 63 the case of CP mixtures with the reentrant phenomenon is left for future studies, it seems that the plot such transformed should follow a “real” S-shaped curve, which might occur also for glycerol if the transformation to the additional, linear  $P_g$  vs  $T_g$  dependence occurred above the hypothetical  $P_g(\text{max}) \approx 7$  GPa. In our opinion the above discussion enforces the conclusion of Ref. 63 that “molecular glasses and colloidal glasses have a common physical interpretation of the way their glass transition changes with temperature and pressure.” On pressurization “temperature-energetic”<sup>63</sup> effects causes the gradual decrease of  $dT_g/dP$ , which may lead to the possible crossover into the hypothetical reentrant liquidization domain. On further compressing the crossover into the hard-sphere-type behavior occurs. In glycerol, the low molecular glass former, the latter takes place before at 6.5 GPa before reaching  $(T_g^{\text{max}}, P_g^{\text{max}})$ . For some molecular glass formers, such as the polymeric liquid crystal P8, the hypothetical maximum may be expected even under a moderate pressure. In bonding-driven network forming materials such as albite or silica, where  $dT_g/dP < 0$ , the hypothetical maximum is hidden under negative pressures, in the isotropically stretched state.

In summary, we hope that this paper pointed out a novel plethora of phenomena which may be revealed when studying the vitrification phenomenon under extreme pressures. The exciting question for the hypothetical general patterns of the glass transition evolution and its controlling in  $P$ - $T$  plane appears. Unusual changes in dynamics, probably associated with nontypical changes of fragility, may be expected on compressing or entering the negative pressure domain. Some of these phenomena may have a significant, but still hidden, influence on properties in the moderate pressure domain, dominated in experiments so far.

## ACKNOWLEDGMENTS

Two of the authors (S.J.R. and C.M.R.) would like to thank the U.S. Naval Research Laboratory for support. One author (A.D.R.) was supported by the Committee for Sci. Res. (KBN, Poland: Grant No. 2PO3B 034 25 for 2003–

2006). Another author (A.R.I.) would like to acknowledge the Bilateral Polish-Hungarian Scientific and Technological Grant (Contract No. PL-10/03) and the Hungarian Research Fund OTKA T 043042.

- <sup>1</sup>E. Donth, *The Glass Transition: Relaxation Dynamics in Liquids and Disordered Material*, Springer Series in Materials Science II (Springer, Berlin, 1998), Vol. 48.
- <sup>2</sup>G. Floudas, *Prog. Polym. Sci.* **29**, 1143 (2004).
- <sup>3</sup>C. M. Roland, S. Hensel-Bielowka, M. Paluch, and R. Casalini, *Rep. Prog. Phys.* **68**, 1405 (2005).
- <sup>4</sup>*Soft Matter Under Exogenic Impacts*, NATO Sci. Series II, edited by S. J. Rzoska and V. Mazur (Springer, Berlin, 2006), Vol. 247.
- <sup>5</sup>M. Paluch, S. J. Rzoska, P. Haldas, and J. Ziolo, *J. Phys.: Condens. Matter* **10**, 4131 (1998).
- <sup>6</sup>M. Paluch, J. Gapiński, and A. Patkowski, *J. Chem. Phys.* **114**, 8048 (2001).
- <sup>7</sup>S. Pawlus, M. Paluch, M. Sekula, J. L. Ngai, S. J. Rzoska, and J. Ziolo, *Phys. Rev. E* **68**, 021503 (2003).
- <sup>8</sup>A. Drozd-Rzoska and S. J. Rzoska, *Phys. Rev. E* **73**, 041502 (2006).
- <sup>9</sup>A. Drozd-Rzoska, *Phys. Rev. E* **72**, 041505 (2006).
- <sup>10</sup>S. P. Andersson and O. Andersson, *Macromolecules* **31**, 2999 (1998).
- <sup>11</sup>A. Gitsas, G. Floudas, and G. Wegner, *Phys. Rev. E* **69**, 041802 (2004).
- <sup>12</sup>R. Casalini and C. M. Roland, *Phys. Rev. E* **69**, 062501 (2004).
- <sup>13</sup>R. Casalini and C. M. Roland, *Phys. Rev. Lett.* **92**, 245702 (2004).
- <sup>14</sup>S. Corezzi, M. Beiner, H. Huth, K. Schoeber, S. Capaccioli, R. Casalini, D. Fioretto, and E. Donth, *J. Chem. Phys.* **117**, 2435 (2002).
- <sup>15</sup>Th. M. Nieuwenhuizen, *Phys. Rev. Lett.* **79**, 1317 (1997).
- <sup>16</sup>V. P. Skripov and M. Z. Faizulin, *Crystal-Liquid-Gas Phase Transitions and Thermodynamic Stability* (Wiley-VCH, Weinheim, 2006).
- <sup>17</sup>T. Grande, S. Stolen, A. Grzechnik, W. A. Crichton, and M. Mezouard, *Physica A* **314**, 560 (2002).
- <sup>18</sup>P. F. McMillan, *High Press. Res.* **23**, 7 (2003).
- <sup>19</sup>G. Jenner, *Mini-Revs. in Organic Chem.* **1**, 9 (2004).
- <sup>20</sup>B. Rodriguez-Spong, Ch. P. Price, A. Jayasankar, A. J. Matzger, and N. Rodriguez-Hornedo, *Adv. Drug Delivery Rev.* **56**, 241 (2004).
- <sup>21</sup>J. Hemley, *Rev. Mineral.* **37**, 671 (1998).
- <sup>22</sup>J.-P. Poirier, *Introduction to the Physics of the Earth's Interior* (Cambridge University Press, Cambridge, 2000).
- <sup>23</sup>E. D. DiMarzio, J. H. Gibbs, P. D. Fleming, and I. C. Sanchez, *Macromolecules* **9**, 763 (1976).
- <sup>24</sup>U. Bengtzelius, W. Goetze, and A. Sjoelander, *J. Phys. C* **17**, 5914 (1994).
- <sup>25</sup>V. Skorudonov and Yu. K. Godovskii, *Polym. Sci., Ser. A Ser. B* **35**, 562 (1993).
- <sup>26</sup>E. Donth and R. Conrad, *Acta Polym.* **31**, 47 (1980).
- <sup>27</sup>R. Lach, W. Grellmann, K. Schroeter, and E. Donth, *Polymer* **40**, 1481 (1999).
- <sup>28</sup>F. E. Simon and G. Glatzel, *Z. Anorg. Allg. Chem.* **178**, 309 (1929).
- <sup>29</sup>S. E. Babb, *Rev. Mod. Phys.* **35**, 400 (1963).
- <sup>30</sup>C. Rein and D. Demus, *Cryst. Res. Technol.* **28**, 273 (1993).
- <sup>31</sup>V. V. Kechin, *J. Phys.: Condens. Matter* **7**, 531 (1995); V. V. Kechin, *Phys. Rev. B* **65**, 05121 (2001).
- <sup>32</sup>L. Burakowsky, D. L. Preston, and R. R. Silbar, *J. Appl. Phys.* **88**, 6294 (2000).
- <sup>33</sup>K. Fuchizaki, Y. Fuji, Y. Ohishi, A. Ohmura, N. Hamaya, Y. Katayama, and T. Okada, *J. Chem. Phys.* **120**, 11196 (2004).
- <sup>34</sup>D. I. Bower, *An Introduction to Polymer Physics* (Cambridge University Press, Cambridge, 2002).
- <sup>35</sup>E. Williams and C. A. Angell, *J. Phys. Chem.* **8**, 232 (1977).
- <sup>36</sup>N. S. Bagdassarov, J. Maumus, B. Poe, A. B. Slutski, and V. K. Bulatov, *Phys. Chem. Glasses* **45**, 197 (2004).
- <sup>37</sup>Z. Trybula and J. Stankowski, *Condens. Matter Phys.* **1**, 311 (1998).
- <sup>38</sup>G. A. Samara and H. Terauchi, *Phys. Rev. Lett.* **59**, 347 (1987).
- <sup>39</sup>G. P. Johari and E. Whalley, *Faraday Symp. Chem. Soc.* **6**, 23 (1972).
- <sup>40</sup>R. L. Cook, H. E. King, Jr., Ch. A. Herbst, and D. R. Herschbach, *J. Chem. Phys.* **100**, 5178 (1994).
- <sup>41</sup>B. L. Schulte and W. F. Oliver III, presented in the Meeting of The American Physical Society, St. Louis, USA, 1996 (unpublished), <http://flux.aps.org/meetings/YR9596/BAPSMAR96/abs/S2480008.html>; W. F. Oliver III, *Mater. Res. Soc. Symp. Proc.* **464**, 21 (1997).
- <sup>42</sup>A. Reiser, G. Kasper, and S. Hunkliger, *Phys. Rev. B* **72**, 094204 (2004); A. Reiser, Ph.D. thesis, Ruprecht-Karls-Universität, Heidelberg, Germany, 2005.
- <sup>43</sup>*Liquids under Negative Pressures*, NATO Sci. Series II, Vol. 84, edited by A. R. Imre, H. J. Maris, and P. R. Williams (Kluwer, Dordrecht, 2002).
- <sup>44</sup>C. A. Angell and Z. Quing, *Phys. Rev.* **39**, 8784 (1989).
- <sup>45</sup>V. P. Skripov and M. Z. Faizullin, *Dokl. Phys.* **46**, 403 (2001).
- <sup>46</sup>L. Landa and K. Landa, *J. Non-Cryst. Solids* **348**, 59 (2004).
- <sup>47</sup>F. H. Stillinger, P. G. Debenedetti, and T. Truskett, *J. Phys. Chem. B* **105**, 11809 (2001).
- <sup>48</sup>M. Utz, P. G. Debenedetti, and F. Stillinger, *J. Chem. Phys.* **114**, 10049 (2001).
- <sup>49</sup>V. N. Novikov and A. P. Sokolov, *Phys. Rev. E* **67**, 031507 (2003).
- <sup>50</sup>P. F. McMillan, *Nat. Mater.* **1**, 19 (2002).
- <sup>51</sup>A. Drozd-Rzoska, S. J. Rzoska, and A. R. Imre, *J. Non-Cryst. Solids* (to be published), special Kia L. Ngai issue.
- <sup>52</sup>F. P. Bundy, *Phys. Rev.* **115**, 274 (1959).
- <sup>53</sup>G. C. Kennedy, A. Jayaraman, and C. Newton, *Phys. Rev.* **126**, 1363 (1962).
- <sup>54</sup>E. Gregoryanz, O. Degtyareva, M. Somayazulu, R. J. Hemley, and H.-K. Mao, *Phys. Rev. Lett.* **94**, 185502 (2005).
- <sup>55</sup>G. W. H. Hoene, *Thermochim. Acta* **332**, 115 (1999); G. W. H. Hoene, S. Rastogi, and B. Wunderlich, *Polymer* **41**, 8869 (2000).
- <sup>56</sup>The value of  $dT_g/dP \approx 2/3$  holds for low molecular organic liquids, molten oxides, and asymmetrical polymers. For symmetrical polymers  $dT_g/dP \approx 1/2$  is recommended.
- <sup>57</sup>K. N. Pham, A. M. Puertas, J. Bergholtz, S. U. Egelhaaf, A. Moussaid, P. N. Pusey, A. B. Schofield, M. E. Cates, M. Fuchs, and W. C. K. Poon, *Science* **296**, 104 (2002).
- <sup>58</sup>S.-H. Chen, W.-R. Chen, and F. Mallamace, *Phys. Rev. E* **66**, 021403 (2002).
- <sup>59</sup>F. Sciortino, *Nat. Mater.* **1**, 1 (2002).
- <sup>60</sup>W. C. K. Poon, *Science* **304**, 830 (2004).
- <sup>61</sup>M. L. Ferrer, C. Lawrence, B. G. Demirjan, D. Kivelson, C. Alba-Simionesco, and G. Tarjus, *J. Chem. Phys.* **109**, 8010 (1998).
- <sup>62</sup>B. V. R. Tata, P. S. Mohanty, and M. C. Valsakumar, *Phys. Rev. Lett.* **88**, 018302 (2002).
- <sup>63</sup>Th. Voigtmann and W. C. K. Poon, *J. Phys.: Condens. Matter* **18**, L465 (2006).